Journal of Sound and Vibration (1996) **197**(3), 351–371

INVESTIGATION OF DAMPING EFFECTS ON STATISTICAL ENERGY ANALYSIS OF COUPLED STRUCTURES

F. F. Yap and J. Woodhouse

Engineering Department, University of Cambridge, Trumpington Street, Cambridge CB2 1PZ, England

(*Received* 14 *June* 1994, *and in final form* 10 *April* 1996)

The effects of damping on energy sharing in coupled systems are investigated. The approach taken is to compute the forced response patterns of various idealised systems, and from these to calculate the parameters of Statistical Energy Analysis model for the systems using the matrix inversion approach [1]. It is shown that when SEA models are fitted by this procedure, the values of the coupling loss factors are significantly dependent on damping except when it is sufficiently high. For very lightly damped coupled systems, varying the damping causes the values of the coupling loss factor to vary in direct proportion to the internal loss factor. In the limit of zero damping, the coupling loss factors tend to zero. This is a view which contrasts strongly with 'classical' SEA, in which coupling loss factors are determined by the nature of the coupling between subsystems, independent of subsystem damping. One implication of the strong damping dependency is that equipartition of modal energy under low damping does not in general occur. This is contrary to the classical SEA prediction that equipartition of modal energy always occurs if the damping can be reduced to a sufficiently small value. It is demonstrated that the use of this classical assumption can lead to gross overestimates of subsystem energy ratios, especially in multi-subsystem structures.

© 1996 Academic Press Limited

1. INTRODUCTION

Statistical Energy Analysis (SEA) is an approach to vibration prediction in complex structures, in which the complete system is broken down into a set of coupled subsystems. The vibration level within each subsystem is characterized by a single number, the mean energy per mode, and energy flow across the junctions between subsystems is characterized by a set of 'coupling loss factors'. There is a simple thermal analogy of SEA, in which subsystem energy plays the role of temperature, and coupling loss factors play the role of thermal conductivities across junctions. The justification of this approach is based on certain exact results in random vibration theory, which may be generalized under certain simplifying assumptions to apply to a wide range of systems (see for example the book by Lyon and DeJong [2] and the review paper by Hodges and Woodhouse [3]).

In the classical developments of SEA (see e.g., references [2, 4]), the coupling loss factors (CLFs) were calculated either by using coupled-oscillator results to represent coupling between modal co-ordinates of the decoupled subsystems, or by using the wave transmission properties of the junctions between subsystems. In either case, the results thus obtained were held to be applicable irrespective of the nature of magnitude of the damping in the subsystems (the couplings being assumed to be conservative). Damping played two roles in this classical theory. It has the obvious effect of removing vibrational energy from

0022–460X/96/430351 + 21 $25.00/0 © 1996 Academic Press Limited

the subsystems, at a rate characterized by the damping loss factors, and it is also an important factor in reducing the statistical variation of the SEA parameters (mean power flows, mean energies, CLFs, etc.) over an ensemble of similar systems (see for example reference [5]). The SEA parameters for members of an ensemble of similar systems differ due to minor differences in structural details. Increasing the damping will in general reduce the variance of the values of these parameters [5]. The explanation is that increasing the damping smooths the frequency response functions of the systems, making them less sensitive to variations in structural details. There are empirical rules that say that the statistical variances are acceptably small if the *modal overlap factors* of the subsystems are greater than a certain value (1·0 is a commonly quoted number). (Modal overlap is defined as the ratio of the damping bandwidth to the average separation of the natural frequencies of the modes; it measures the 'smoothness' of the frequency response function. A high modal overlap factor implies either high damping or high modal density, or both).

In the classical development of SEA, a number of assumptions are usually made about the nature of the subsystems and their coupling. With these assumptions, the basic linear energy-flow equations of SEA can be derived. However, when one comes to apply SEA in practice it is generally far from clear which of these assumptions are reasonable and which are violated, and if some assumptions are violated it is then far from clear whether the model predictions will be in error, and if so in which direction and by how much. A large literature has built up around such questions (see e.g., references [2, 5–15]).

In this paper a different approach is taken to SEA modelling, which circumvents most of these issues. From an explicit model of a complete, coupled, system one can compute the response at any given point to driving at any other point. With this known, it is straightforward to perform a numerical version of the now-standard experimental procedure of inverse measurement of SEA parameters [1, 16]. The pattern of subsystem energy responses, in the appropriate SEA sense, can be calculated for a given energy input to one particular subsystem (by assuming, for example, 'rain-on-the-roof' excitation there). Given these patterns for all possible excitation subsystems, and on assuming only that the driving on separate subsystems is uncorrelated in time, the parameters of an SEA model follow by simple matrix inversion (provided certain conditions on the matrix coefficients are satisfied [1, 14, 16]. In this way, a full set of coupling loss factors can be obtained, in terms of which the SEA model gives the response exactly, without any assumptions of weak coupling, diffuse wavefields and so on.

The questions of interest then concern how the values of these (formally exact) coupling loss factors relate to those obtained by the classical procedures of modal coupling or wave transmission. Two issues in particular merit discussion. First, non-zero coupling loss factors may be found for subsystems which are physically remote. Such 'indirect coupling' has been discussed in several papers in recent years [3, 17, 18]. The second issue, which is the main focus of this paper, concerns the role of damping. There is no *a priori* reason to expect the coupling loss factors, thus computed, to be independent of damping, and it will shortly be demonstrated that strong dependence on subsystem damping is indeed usually found. The physical significance of this dependence will be explored, and it will be argued that classical SEA modelling can often be augmented relatively simply to allow for the main consequence of this dependence. The result is to extend the range of useful SEA prediction to lower levels of modal overlap than has been possible hitherto.

A useful starting point is to examine qualitatively how a relation between internal loss factor and coupling loss factor can affect the energy distribution in a two-subsystem structure. This can be done by analogy with heat transfer between two coupled thermal bodies (see Figure 1). The heat flow from one body to another is proportional to their temperature difference $\theta_1 - \theta_2$. At equilibrium, all the energy that is transferred to body

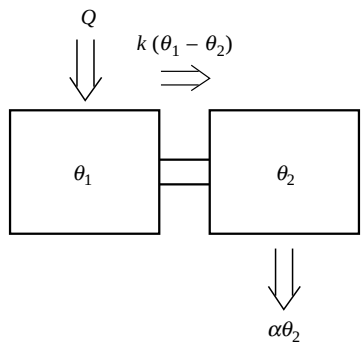

Figure 1. Heat flow analogy.

2 will be dissipated, the rate of dissipation being proportional to θ_2. Thus $k(\theta_1 - \theta_2) = \alpha\theta_2$, where k and α are the heat transfer coefficient and dissipation factor respectively. The ratio of the temperatures is then given by

$$\theta_1 / \theta_2 = 1 + \alpha/k. \tag{1}$$

It can be seen from equation (1) that when α is much greater than k the temperature of body 1 is much higher than that of body 2. This is because the dissipation in 2 will be high, so the temperature difference must be great enough to create a high heat flow to 2. If the dissipation factor is reduced, then the temperature ratio will also be reduced. When α becomes much smaller than k, there will only be a small temperature difference to maintain the power flow needed to compensate for the small heat loss in 2. In the limit of zero dissipation, the temperatures of the two bodies will be equal.

According to SEA, vibration transmission in a two — subsystem structure is analogous to heat transfer if modal energy is regarded as the 'temperature' of the system (see Figure 2). The internal loss factor (or damping factor) is similar to the dissipation factor α, and the coupling loss factor is the mechanical equivalent of the heat transfer coefficient k. Under various conditions, one can therefore expect energy sharing to behave in a similar manner to the case of heat transfer described above. When the internal loss factor in the structure is high compared to the coupling loss factor, the modal energy of subsystem 2 will be much smaller than that of subsystem 1. Reducing the damping in the system will decrease the ratio of the modal energies $e_1 : e_2$. As the damping factor approaches zero, one expects the ratio of the modal energies to become 1. This condition is known as *equipartition of modal energy*. It means that the modal energies of the subsystems are

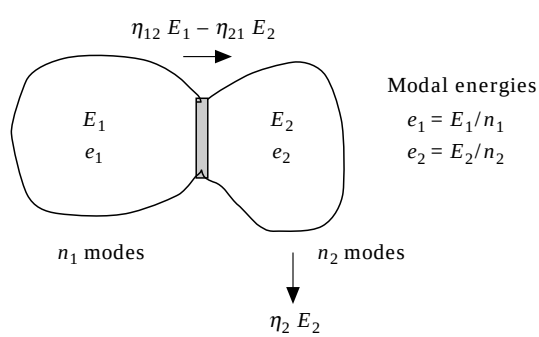

Figure 2. SEA power flow model.

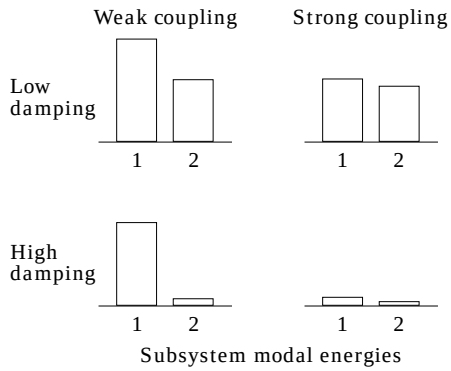

Figure 3. Vibrational energies for various combinations of coupling and damping strength.

approximately equal when the damping in the structure is very weak. The relation between the modal energies under different conditions of damping and coupling are summarized graphically in Figure 3 (adapted from reference [1]).

The condition of equipartition of modal energy suggests that the use of SEA for power flow analysis is not necessary when the damping in the structure is sufficiently low, since one could then expect energy to be more or less equally distributed among the subsystems. With high damping (or high modal overlap) SEA is known to work well, in the sense that the predictions made by SEA for a 'typical' member of an ensemble of similar systems yield mean values whose variances are acceptably small. The main area of uncertainty would thus seem to be when damping is moderate, in some suitable sense.

In this paper, the effects of damping on energy sharing in coupled systems are investigated within the framework of SEA. In particular it will be shown that the values of the coupling loss factors are strongly dependent on damping except when it is sufficiently high. It will also be shown that in the limit of zero damping the coupling loss factors tend to zero. One of the implications of this is that the tendency towards equipartition of modal energy under low damping/low modal overlap does not occur in general. The results will be demonstrated by using finite element models of coupled beams and plates.

2. GLOBAL – MODE APPROACH

It can be shown that the SEA parameters of mean energies, input powers, power flows and coupling loss factors can be expressed in terms of the velocity frequency response function, $H(r, s, \omega)$, of the structure (see Appendix A). The frequency response function can in turn be derived if the *global modes* and natural frequencies of the structure are known. The global modes are the modes of the entire structure: the set of coupled subsystems and the couplings. Each global mode contains information about the motion of every coupled subsystem.

The global-mode approach is different from the model approach normally used in classical SEA. In the classical modal aproach, the individual subsystem responses are described in terms of their *uncoupled* or '*blocked*' modes, defined by isolating that subsystem from the others in some suitable way (see e.g., chapter 3 of reference [2], and reference [15]). One might ask why it is necessary to derive the SEA parameters when the global modes are already known. The point is that we are not here concerned with the prediction of structural response as such, we are performing numerical experiments on

systems to determine whether and how the SEA parameters depend on the damping of the systems. The global-mode approach gives a convenient way to study such issues.

In terms of the global modes ψ_j and undamped natural frequencies ω_j, the velocity frequency response function $H(r, s, \omega)$ is

$$H(r, s, \omega) = \sum_{j=1}^{\infty} \psi_j(r)\psi_j(s)H_j(\mathrm{i}\omega), \qquad H_j(\mathrm{i}\omega) = \mathrm{i}\omega/(-\omega^2 + \beta_j\,\mathrm{i}\omega + \omega_j^2). \qquad (2, 3)$$

$H_j(\mathrm{i}\omega)$ is the modal frequency response function and β_j is the damping factor associated with mode j. In using the modal summation method, it is assumed here that the overall damping behaviour of the system can be adequately represented with a damping matrix which is diagonal in normal (modal) co-ordinates. This condition restricts the generality of the systems considered but is usually a good approximation if damping is small. For convenience of calculation, it will sometimes be assumed that all the β_j are equal: this may not be too far from the truth in practice when the subsystems have similar construction and materials. In any case, one does not usually know how damping is distributed, and this assumption does not appear to detract seriously from the usefulness of the results to be derived.

Upon substituting equation (3) into equation (A1), the mean energy, E_{pq}, of subsystem p when subsystem q is subjected to 'rain-on-the-roof' excitation is found to be

$$E_{pq} = m_p S_q \sum_{j=1}^{\infty}\sum_{k=1}^{\infty} \int_p \psi_j(r)\psi_k(r)\,\mathrm{d}r \int_q \psi_j(r)\psi_k(r)\,\mathrm{d}r \int_\Omega H_j(\mathrm{i}\omega)H_k^*(\mathrm{i}\omega)\,\mathrm{d}\omega, \qquad (4)$$

where $\int_p \cdot\cdot\,\mathrm{d}r$ represents a line/surface/volume integral, as appropriate to the nature of the subsystem. S_q is the mean-square spectral density (assumed constant) of the excitation which is band-limited to the frequency range Ω, and m_p is the mass of subsystem p per unit length/area/volume. Similarly, from equation (A2), the input power to subsystem q is

$$\Pi_q = S_q \sum_{j=1}^{\infty} \int_q \psi_j^2(r)\,\mathrm{d}r \int_\Omega \mathrm{Re}[H_j(\mathrm{i}\omega)]\,\mathrm{d}\omega. \qquad (5)$$

For pure white noise excitation, $\Omega = -\infty \cdots +\infty$, the integrals $\int_\Omega H_j(\mathrm{i}\omega)H_k^*(\mathrm{i}\omega)\,\mathrm{d}\omega$ and $\int_\Omega \mathrm{Re}[H_j(\mathrm{i}\omega)]\,\mathrm{d}\omega$ can be expressed in standard forms and evaluated by using tables (e.g. [19]). When the excitation is band-limited so that Ω is finite, the integrals are more complicated but closed form solutions still exist. The results are given in Appendix B. Note that only the real parts of the integrals need to be evaluated since the sum of all imaginary parts is equal to zero (because $\int_\Omega H_j(\mathrm{i}\omega)H_k^*(\mathrm{i}\omega)\,\mathrm{d}\omega$ is the complex conjugate of $\int_\Omega H_k(\mathrm{i}\omega)H_j^*(\mathrm{i}\omega)\,\mathrm{d}\omega$).

Hence, if the global mode shapes and natural frequencies are known, equations (4) and (5) can be used to evaluate the subsystem energies and input powers. From these, the coupling loss factors of the subsystems can be derived by using the matrix-inversion technique given by equation (A4). For a structure with only two coupled subsystems (see Figure 4), the coupling loss factors are

$$\eta_{12}\,\bar{\omega} = \Pi_2 E_{21}/(E_{11}E_{22} - E_{12}E_{21}), \qquad \eta_{21}\,\bar{\omega} = \Pi_1 E_{12}/(E_{11}E_{22} - E_{12}E_{21}), \qquad (6)$$

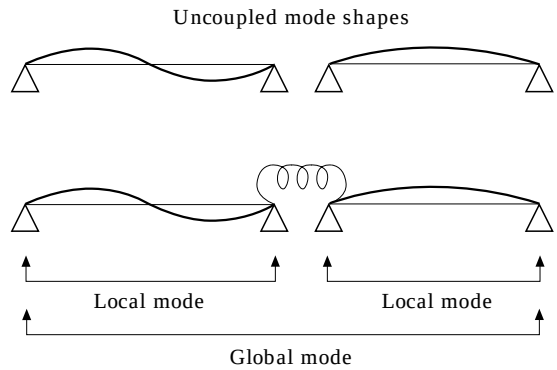

Figure 4. Global, local and uncoupled modes.

and the internal loss factors are given by

$$\eta_1\,\bar{\omega} = (\Pi_1\,E_{22} - \Pi_2\,E_{21})/(E_{11}\,E_{22} - E_{12}\,E_{21}),$$
$$\eta_2\,\bar{\omega} = (\Pi_2\,E_{11} - \Pi_1\,E_{12})/(E_{11}\,E_{22} - E_{12}\,E_{21}), \tag{7}$$

where $\bar{\omega}$ is the centre frequency of the excitation band.

One advantage of using the modal summation method is that the effects of damping can be conveniently studied. Changing the modal damping factors will only change the values of the integrals $\int_\Omega H_j\,(\mathrm{i}\omega)H_k^*\,(\mathrm{i}\omega)\,\mathrm{d}\omega$ and $\int_\Omega \mathrm{Re}[H_j\,(\mathrm{i}\omega)]\,\mathrm{d}\omega$. All the other terms in equations (4) and (5) will remain unaffected.

3. ESTIMATING CLF BY USING F.E. MODELS

Except for the simplest of cases where the mode shapes can be easily deduced, it is difficult to evaluate equations (4) and (5) analytically because of the number of summations and integrations involved. However, the equations can be easily implemented as a computer algorithm and the integrals and summations can be evaluated numerically. The mode shapes and natural frequencies can be obtained from a finite element analysis of the structure concerned. The main advantage of using finite element models in the study of SEA is that the details of the models can be easily varied. By varying the geometric and material properties of the models we can investigate how the SEA parameters will vary. The major limitation of the method is that the junctions may be very difficult to model. Also, if the modal density of the structure is high, a large number of modes will have to be extracted. But in most cases, computer experiments done on F.E. models are more flexible, less time consuming and more controllable than experiments carried out on laboratory models of the real structures. Note that F.E. analysis is used here *not* as a predictive tool to estimate structural response, but as a means of investigating the characteristics of the SEA parameters. The accuracy of the mode shapes and eigenvalues extracted from the model is not of crucial importance here. The main issue of interest is how the SEA parameters will behave as the various properties (e.g. damping and boundary conditions) of the model are varied.

3.1. CASE STUDIES: COUPLED PLATES AND BEAMS

In this section, the coupling loss factors are derived for a pair of coupled beams and a pair of coupled plates. The first system (see Figure 5), consists of two simply supported aluminium beams coupled together at one end by a rotational spring. The beams are of

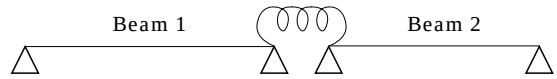

Figure 5. Two beams coupled by a rotational spring. Spring constant = 2·5 Nm/rad; bending stiffness, $EI = 0{\cdot}424$ Nm, mass/unit length, $m = 0{\cdot}065$ kg/m; length of beam 1, $l_1 = 1{\cdot}0$ m; length of beam 2, $l_2 = 0{\cdot}7$ m.

different length but the other properties are the same. The second system (see Figure 6) is made up of two irregularly shaped flat aluminium plates of different thickness welded together at one edge. The plates are simply supported at the corners. The systems can be modelled by using the appropriate finite elements and applying the proper constraints. The undamped mode shapes and natural freuqencies can then be obtained by using a F.E. mode extraction method such as the Lanczos method or the subspace method. Care must be taken to ensure that the details of the F.E. models are sufficiently fine so that the errors in the mode shapes and eigenvalues are not too big, especially for the higher frequency modes. One way of checking this is to refine the mesh density of the F.E. model progressively, and compare the eigenvalues obtained from the different models. This is carried out until the differences between the eigenvalues are acceptably small.

The mode shapes and eigenvalues thus obtained are then used to determine the coupling loss factors according to equations (4–6). One source of errors in the computation of CLFs comes from modal truncation. Since only a finite number of modes can be extracted, the summation $\Sigma_{j=1}^{\infty}$ can only be approximated by $\Sigma_{j=1}^{N}$. But if the eigenvalues of the excluded modes are much greater than those within the frequency band of excitation Ω, then the contribution from these non-reverberant modes can be safely ignored.

For simplicity, the modal damping factors of the sytems, β_j are assumed to be equal, $\beta_j = \beta_0$. By computing the coupling loss factors for different values of β_0, one can investigate the dependence of CLF on damping. It can also be shown that, as expected, the internal loss factors η_1 and η_2 of the subsystems are equal to each other and to $\beta_0/\bar{\omega}$. This is true for any choice of excitation band because all the modes are equally damped.

The coupling loss factors for the coupled beams (for a given excitation band) are plotted against the internal loss factors in Figure 7. The corresponding results for the coupled plates are shown in Figure 8. From the graphs, one feature stands out immediately: the coupling loss factors are strongly sensitive to variation in damping below a certain value of the internal loss factor. Also plotted on the graphs are the values of the CLF as predicted by the wave approach (see references [20, 21] for a detailed exposition of the wave approach). The wave estimates do not take damping effects into account and it can be seen that their values can deviate a lot from the 'true' values. Roughly, the graphs can be divided into three regions of interest: a linear region, a flat region and a transition region in

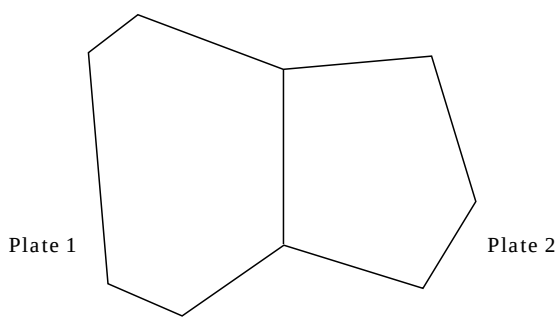

Figure 6. Two coupled plates with a linear junction. Plate 1: area, $A_1 = 1{\cdot}74$ m^2, thickness, $t_1 = 3{\cdot}22$ mm, mass/area, $m_1 = 9{\cdot}56$ kg/m^2; plate 2: area, $A_2 = 1{\cdot}0$ m^2, thickness, $t_2 = 1{\cdot}0$ mm, mass/area, $m_2 = 2{\cdot}97$ kg/m^2.

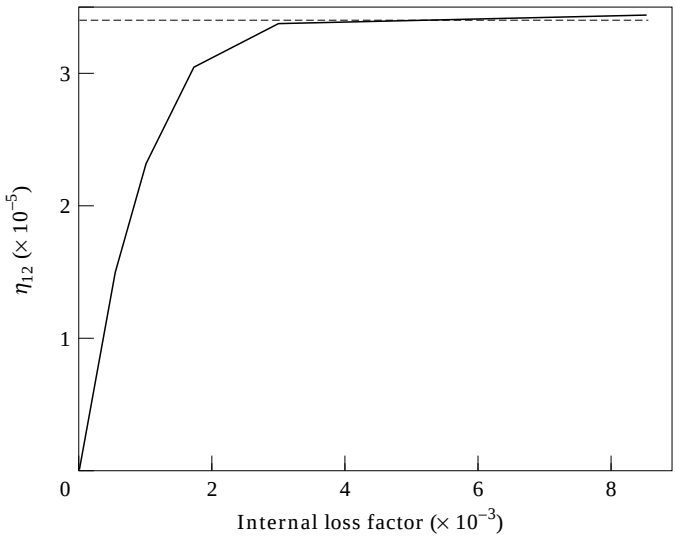

Figure 7. Coupling loss factors for coupled beams (2560–5100 Hz) ——, Modal approach; – – –, wave approach.

between. When the damping is high, the CLFs are quite insensitive to changes in the damping. This is the familiar region in which the variances of the SEA parameters are known to be small. The average values of the CLF in this region tend to agree well with the values predicted by the wave technique. As the damping is reduced, there comes a point below which there is a rapid drop in the values of the CLF. Eventually, as the damping approaches zero, the coupling loss factors also approach zero and the dependence on damping becomes almost linear.

The graphs also illustrate the common observation that the wave method tends to *overestimate* the coupling loss factors. For instance, experiments carried out by Fahy and Mohammed [5] on coupled beam and plate systems have shown that the wave estimates

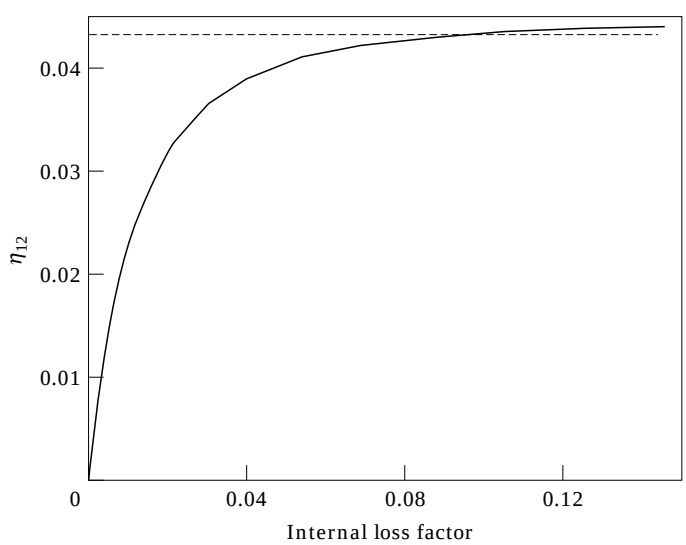

Figure 8. Coupling loss factors for coupled plates (1·6–110 Hz). Key as Figure 7.

of coupling loss factors generally exceed the actual values when the average modal overlap factor is much less than unity. The values predicted by the wave method correspond to upper limits that lie in the plateau region of the coupling loss factor-internal loss factor curve.

4. EFFECTS OF DAMPING ON SEA PARAMETERS

In this section it is shown that the coupling loss factor, when calculated by the inverse method, is linearly dependent on the damping factor when the damping is small, and that it approaches zero in the limit of very weak damping. In this argument one implicitly assumes that one is not dealing with a very special case, such as that of identical subsystems. It is known that such cases can sometimes have a disproportionate influence on the ensemble-averaged system properties [22, 23]. The authors are here seeking to examine the properties of a *typical* member of the ensemble of systems, leaving these special cases aside. The resulting prediction of the coupling loss factor is representative of the *mode* rather than the mean of the statistical distribution, a more useful quantity for practical purposes.)

It can be seen from equation (4) that the terms which provide for the damping effects on the subsystem energy E_{pq} are

$$\mathrm{Re}\left[\int_{\Omega} H_j\,(\mathrm{i}\omega)H_k^*\,(\mathrm{i}\omega)\,\mathrm{d}\omega\right] = \mathrm{Re}\left[\int_{\Omega} \frac{\mathrm{i}\omega}{-\omega^2+\beta_j\,\mathrm{i}\omega+\omega_j^2} \times \frac{-\mathrm{i}\omega}{-\omega^2-\beta_k\,\mathrm{i}\omega+\omega_k^2}\,\mathrm{d}\omega\right]. \quad (8)$$

(Only the real parts need be considered because the imaginary parts sum to zero.) This integral can be evaluated in closed form for any combination of Ω, ω_j, ω_k, β_j and β_k (see Appendix A). In Figure 9 the values of the integral are plotted against frequency, for modes that lie inside the frequency band of excitation. When the damping factors are small, the values of the integral for $j = k$ are much greater than for $j \neq k$. This means that the energy

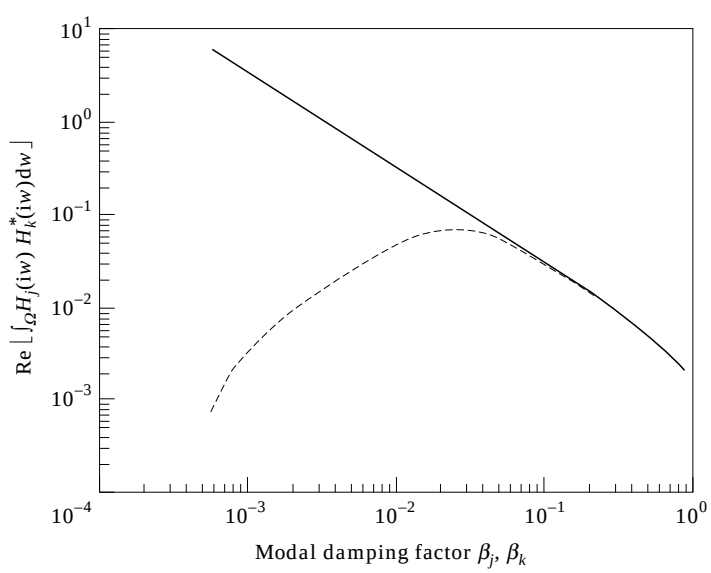

Figure 9. $\mathrm{Re}[\int_\Omega H_j(\mathrm{i}\omega)H_k^*(\mathrm{i}\omega)\,\mathrm{d}\omega]$ versus Modal damping factors ($\beta_j = \beta_k =$ constant; $\omega_j, \omega_k \in \Omega$), ——, $j=k$; – – –, $j \neq k$.

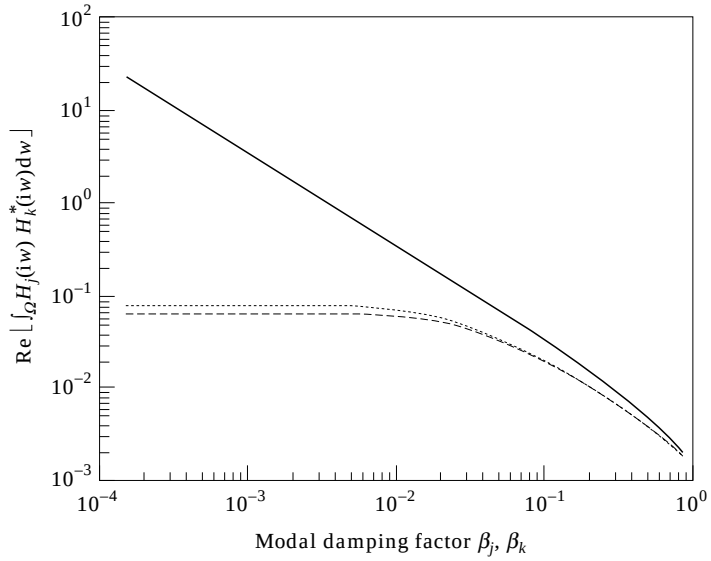

Figure 10. Re[$\int_\Omega H_j(\mathrm{i}\omega)H_k^*(\mathrm{i}\omega)\,\mathrm{d}\omega$] versus Modal damping factors ($\beta_j = \beta_k =$ constant) ——, $j=k(\omega_j, \omega_k \in \Omega)$; – – –, $j \neq k(\omega_j, \omega_k \notin \Omega)$; · · · ·, $j = k(\omega_j, \omega_k \notin \Omega)$.

of the subsystem will come mainly from what one may term the *coherent* response of the modes. This can be explained by the fact that, when the damping is small, the modal frequency response functions have very narrow peaks and there is very little modal overlap between the modes. The incoherent (i.e. $j \neq k$) response of the modes is then insignificant compared to the coherent response.

Also, for small damping, the values of the integral for modes lying outside the band Ω will be much smaller than that for modes within the band: see Figure 10. This is expected because modes outside the band are hardly excited when the damping is small. The contribution to the energy from the non-reverberant response is therefore insignificant.

Hence for small damping the subsystem energy E_{pq} can be approximated by

$$E_{pq} \approx m_p S_q \sum_{\substack{j \\ \omega_j \in \Omega}} \int_p \psi_j^2(r)\,\mathrm{d}r \int_q \psi_j^2(r)\,\mathrm{d}r \int_\Omega |H_j(\mathrm{i}\omega)|^2\,\mathrm{d}\omega. \tag{9}$$

Note that all the terms due to non-coherent ($j \neq k$) and non-reverberant ($\omega_j \notin \Omega$) modal responses have been excluded. The integral $\int_\Omega |H_j(\mathrm{i}\omega)|^2\,\mathrm{d}\omega$ for small β_j can be approximated by taking the integration limits from $-\infty$ to $+\infty$. This can be shown to be equal to π/β_j (see Appendix 1 of reference [24]). Hence, the energy of the subsystem is inversely proportional to the damping factor,

$$E_{pq} \approx \pi m_p S_q \sum_{\substack{j \\ \omega_j \in \Omega}} \int_p \psi_j^2(r)\,\mathrm{d}r \int_q \psi_j^2(r)\,\mathrm{d}r \frac{1}{\beta_j} \approx \left(\frac{\pi m_p S_q}{\overline{\beta}}\right) \sum_{\substack{j \\ \omega_j \in \Omega}} \int_p \psi_j^2(r)\,\mathrm{d}r \int_q \psi_j^2(r)\,\mathrm{d}r, \tag{10}$$

where $\overline{\beta}$ is the average value (weighted) of the modal damping factors. If all the modal damping factors are equal, then $\overline{\beta} = \beta_j$.

Similarly, from equation (5), the input power Π_q can be shown to be

$$\Pi_q \approx \pi S_q \sum_{\substack{j \\ \omega_j \in \Omega}} \int_q \psi_j^2 (r)\, \mathrm{d}r \tag{11}$$

when the damping is small. Note that the input power is independent of damping. This is similar to the well known result that the input power to an oscillator excited by white noise of mean-square spectral density S_0 is $\pi S_0 / m$ (see, for example, reference [2]). Substituting equations (10) and (11) into the expression (6) for the coupling loss factor η_{pq} gives

$$\eta_{pq} \approx \frac{\sum_j \sum_k P_j Q_j Q_k}{\sum_j \sum_k P_j Q_k (P_j Q_k - P_k Q_j)} \frac{\bar{\beta}}{\bar{\omega}}, \tag{12}$$

where

$$P_j = m_p \int_{\text{subsystem } p} \psi_j^2 (r)\, \mathrm{d}r, \qquad Q_j = m_q \int_{\text{subsystem } q} \psi_j^2 (r)\, \mathrm{d}r,$$

and the summations include the reverberant modes only ($\omega_j, \omega_k \in \Omega$).

Also, substituting equations (10) and (11) into equation (7) gives

$$\eta_1 \approx \eta_2 \approx \bar{\beta}/\bar{\omega}. \tag{13}$$

Hence for small damping the coupling loss factor is directly proportional to the internal loss factor, as was seen in Figures 7 and 8. The gradient of the linear region of the CLF-ILF graph is equal to the coefficient of $\bar{\beta}/\bar{\omega}$ in equation (12). Note that this is completely defined by the mode shapes only and does not involve the eigenvalues of the systems. In general, the value of the gradient reflects the strength of the coupling between the subsystems. Weakly coupled systems have low gradients, and steep gradients are usually associated with strong couplings.

The above analysis can readily be generalized to a system with any number of coupled subsystems, with the same conclusion, that CLFs are directly proportional to internal loss factor when the damping is small. (As before, this conclusion depends on the fact that the system under consideration is not in anomalous special case, such as one with identical subsystems.)

5. ENERGY FLOW AND EQUIPARTITION OF ENERGY

Figures 11 and 12 show the ratios of the subsystem modal energies plotted against the internal loss factors for the coupled-beam and coupled-plate systems respectively. In each case, only one subsystem is excited. The solid curves show the ratio of the modal energy of subsystem 2 to that of subsystem 1 when only subsystem 1 is excited. The dotted curves show the reverse situation, with only subsystem 2 excited. In each case, it can be seen that as the damping is decreased the ratio increases but, interestingly, never approaches unity in the limit of zero damping. In this particular case the values of the ratio at zero damping are quite small, showing that the modal energy of the directly excited subsystem remains

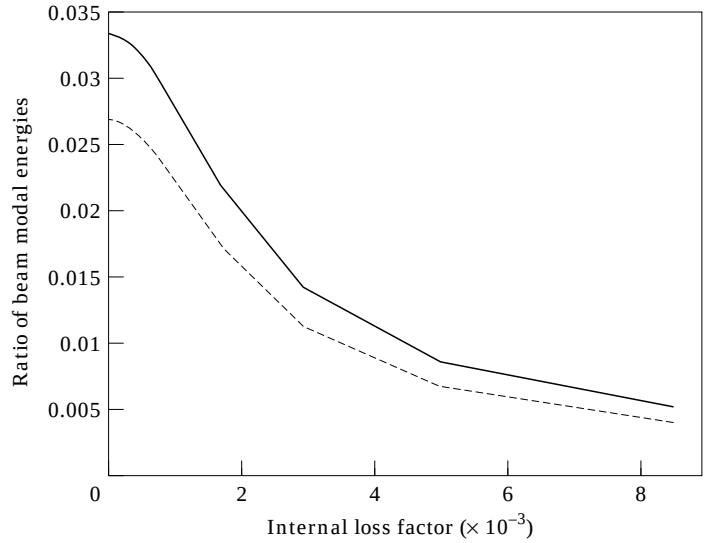

Figure 11. Ratio of modal energies for coupled beams. ——, e_{21}/e_{11} (beam 1 excited); – – –, e_{12}/e_{22} (beam 2 excited).

substantially bigger than that of the indirectly excited subsystem. This result is contrary to the classical SEA prediction that equipartition of modal energy always occurs at small damping or modal overlap. This behaviour can be seen as a direct consequence of the fact, discussed in the previous section, that the response is governed by the coherent response of individual global modes: the modal energy ratio as damping goes to zero represents a kind of average of the global modes within the frequency band, dominated by those having large amplitude in the driven subsystem.

Recall that the argument for equipartition of modal energy is based on the heat flow analogy given in section 1. The conclusion of equal distribution of 'temperature' (modal energy) when dissipation is small is drawn from equation (1),

$$\theta_1/\theta_2 = 1 + \alpha/k,$$

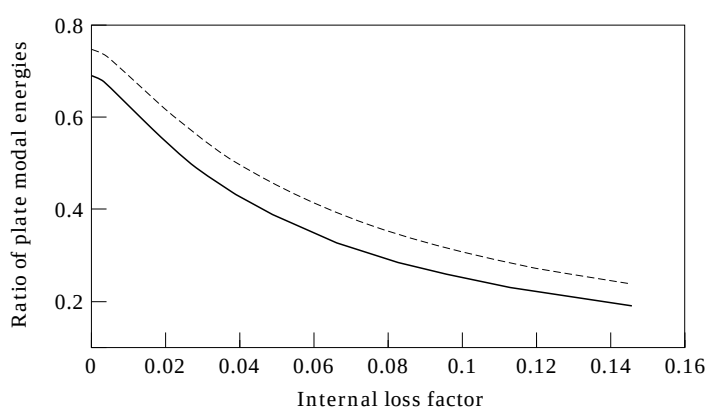

Figure 12. Ratio of modal energies for coupled plates. ——, e_{21}/e_{11} (plate 1 excited); – – –, e_{12}/e_{22} (plate 2 excited).

whereby $\theta_1 = \theta_2$ when the heat dissipation factor α goes to zero. The analogous equation for vibration transmission would be

$$e_{11}/e_{21} = 1 + \eta_2/\eta_{21}.$$

One can now see that this analogy argument is flawed because, unlike the heat transfer coefficient k, the coupling loss factor η_{21} is proportional to the loss factor η_2 when damping is small, so that the ratio $\lim_{\eta_2 \to 0} \eta_2/\eta_{21}$ is a non-zero constant. Hence equipartition of energy is never attained.

The implication of this is that, when the damping is light, SEA predictions of energy distribution based on the wave approach will overestimate the modal energy of the non-directly excited subsystem (except perhaps for special cases, such as those with identical subsystems). (The meaning of light damping depends on the extent of the linear region of the CLF versus Loss factor curve. It generally refers to the situation when the modal overlap factors are small.) Further, for multi-subsystem structures connected in a chain, the predictions will become progressively worse down the chain. This effect will be demonstrated by an example in section 6.

Equipartition of energy can be approximately attained if the ratio η_2/η_{21} is small. Graphically, this means that the slope of the linear region of the CLF versus Internal loss factor curve should be high. So, in a sense, the strength of the coupling between a pair of subsystems should be measured by the value of the gradient given in equation (12), rather than by the actual values of the CLFs.

It is also interesting to see how the energy flow across the coupling is affected by reducing the damping in the subsystems. Figures 13 and 14 show the power flows for the coupled beams and coupled plates respectively (normalized to unit input power). One sees that the power flow across the joint increases as damping decreases. Eventually, as damping approaches zero, the power flow becomes constant. This can be deduced from considering the power flow equation

$$P_{12} = \eta_{12} E_{11} - \eta_{21} E_{21} = \eta_{12} E_{11} (1 - e_{21}/e_{11}).$$

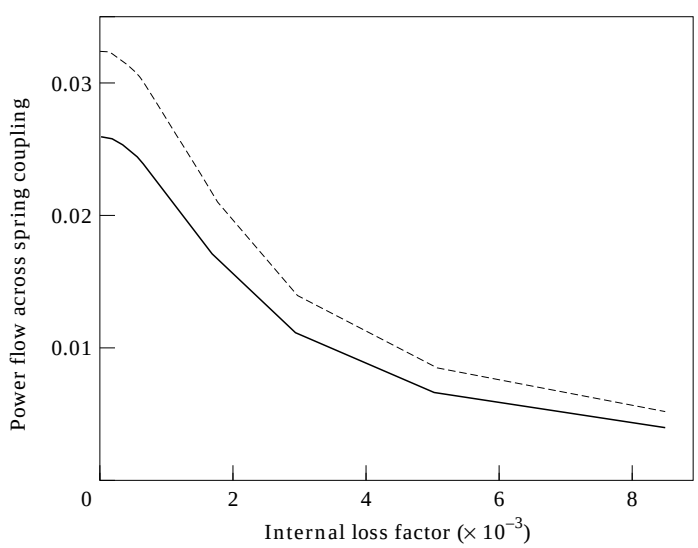

Figure 13. Normalized power flow across spring coupling of coupled beams. ——, P_{12} (beam 1 excited); – – –, P_{21} (beam 2 excited).

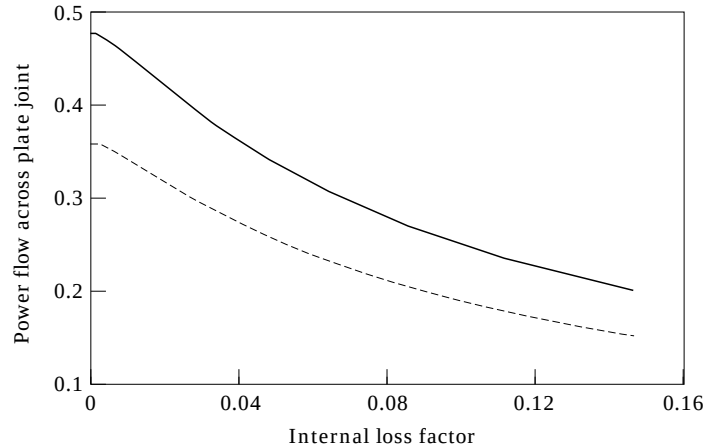

Figure 14. Normalized power flow across plate joint. ——, P_{12} (plate 1 excited); – – –, P_{21} (plate 2 excited).

From equations (10) and (12), the product $\eta_{12} E_{11}$ is constant when damping approaches zero. Also, equipartition of energy does not occur, so the term within brackets is non-zero. Hence the power flow is a finite constant.

The strong dependence of CLFs on damping may also contribute to the high variance in SEA predictions at low modal overlap. At low modal overlap, the CLFs are sensitive to small changes in the damping, and so the CLFs for an ensemble of lightly damped systems will have a high variance about the mean value. This in turn implies that the predictions of subsystem energies and power flows based on the average value of the CLFs will have high variances as well.

6. ENERGY SHARING IN THREE COUPLED PLATES

To conclude the energy predictions made by using the wave approach are compared with those from the global-mode approach, for a multi-subsystem structure. Figure 15 shows a system consisting of three coupled plates simply supported at the corners. The plates are irregular in shape and have different thicknesses and areas. The material properties of the plates are the same (aluminium). Figures 16 and 17 show the variation of the coupling loss factors η_{12} and η_{23} (for transverse vibration) with respect to the internal loss factors. The solid curves represent CLF values (averaged over the frequency band) obtained from the global-mode approach described in section 2. The mode shapes and eigenvalues of the system were extracted by finite element modal analyses. The dotted curves represent CLF values predicted by the wave approach. In the wave approach one derives the CLF from

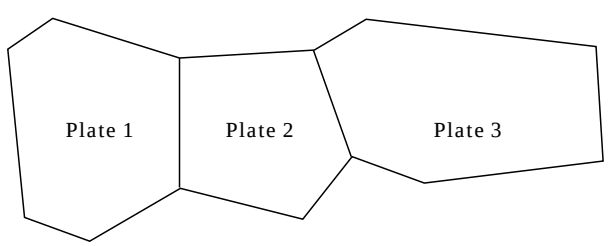

Figure 15. Three coupled aluminium plates. Plate 1: area, $A_1 = 1{\cdot}74$ m^2, thickness, $t_1 = 3{\cdot}22$ mm; plate 2; area, $A_2 = 1{\cdot}0$ m^2, thickness, $t_2 = 1{\cdot}0$ mm; plate 3: area, $A_3 = 2{\cdot}0$ m^2, thickness, $t_3 = 4{\cdot}0$ mm.

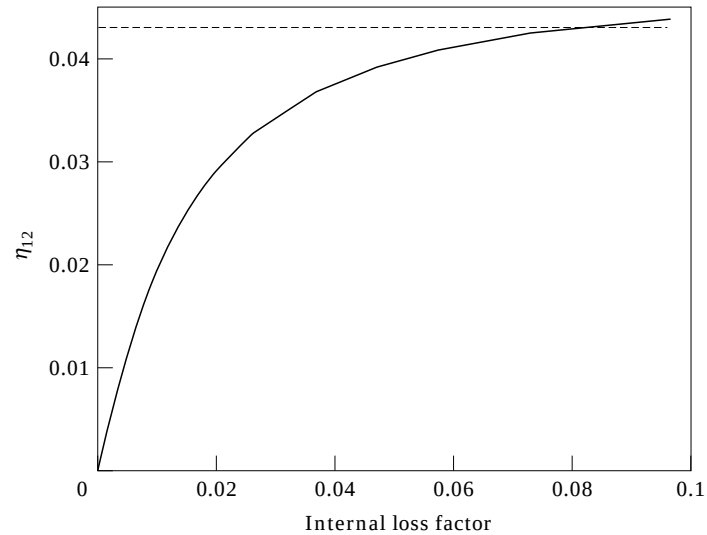

Figure 16. Coupling loss factors η_{12} between plate 1 and plate 2. ——, Modal approach; – – –, wave approach.

the transmission and reflection coefficients of the joints (which in this case are jumps in the plate thickness, symmetric about the middle surface of both plates). This does not take into account the boundary conditions and damping of the plates (see references [20, 21]). Hence, the values of the CLFs are independent of the internal loss factors.

There are at least four possible reasons for the discrepancies between the wave approach and the modal approach. Firstly, in the wave approach one assumes total incoherence of the waves propagating in different directions. In reality, the boundary conditions of the finite system will always introduce some coherence effects, and these may be amplified as the damping is decreased. Secondly, the wave estimate of the CLF is derived from the transmission coefficients of the joint, averaged over all angles of incidence. This may include too big a contribution from near-grazing angles, not actually well represented in

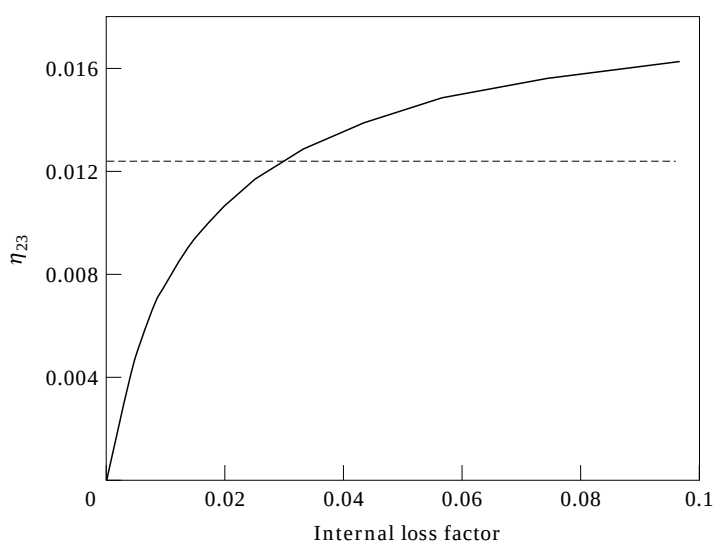

Figure 17. Coupling loss factor η_{23} between plate 2 and plate 3. ——, Modal approach; – – –, wave approach.

the global modes. Thirdly, the existence of a third coupled plate changes the response of the first two plates, but this is not taken into consideration by the wave method. Fourthly, in the wave approach one ignores the contribution to the subsystems responses from the evanescent components of the transmitted and reflected waves at the joints (and at the points of excitation). If the damping is weak the effects of the evanescent waves will be negligible compared to the propagating waves since they decay rapidly. But with high damping, the decay rate of the 'propagating' waves will become faster so that the contribution from the evanescent components may become relatively more significant.

The CLFs obtained from both methods are used to predict the energies of the plates when plate 1 is subjected to 'rain-on-the-roof' pressure forces within the frequency band 10–700 rad/s. The energies can be obtained by inverting equation (A3). Figure 18 shows the ratios of the modal energy of plate 2 to the modal energy of plate 1, e_{21}/e_{11}. It can be seen that the wave predictions deviate from the modal predictions as damping is decreased. The wave estimates tend towards unity, indicating equipartition of energy. The values of the ratio as given by the modal approach are substantially smaller. Figure 19 shows the ratios of the modal energy of plate 3 to that of plate 1, e_{31}/e_{11}. The differences between the two predictions are even greater, especially for very light damping. Whereas the wave approach predicts the modal energies to be equal at zero damping (equipartition), the actual value of the modal energy of plate 3 in less than half that of plate 1. Another way of interpreting the results is that applying more damping to lightly damped coupled systems may cause *less* decrease in the energy ratio than expected.

The above case study highlights some of the pitfalls involved in using the wave approach to estimate energy sharing in lightly damped systems. The wave approach tends to overestimate the CLF in these cases, leading to overestimated values for the energy in the non-directly excited subsystems. It is important to realize that coupling loss factors measure not only the actual strength of the couplings, but also the magnitude of the damping in the subsystems.

The term 'lightly damped' is used loosely here to refer to that portion of the CLF versus Loss factor curve where the gradient is high. The absolute values of the loss factors in this

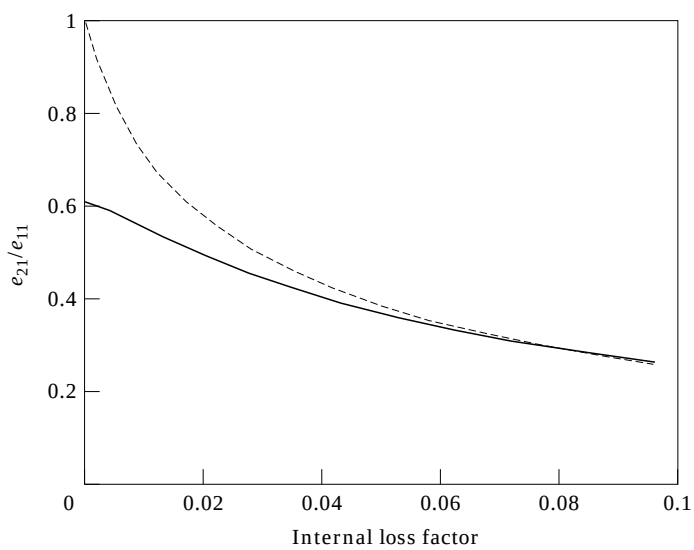

Figure 18. Ratio of modal energies e_{21}/e_{11} between plate 2 and plate 1. ——, Modal approach; – – –, wave approach.

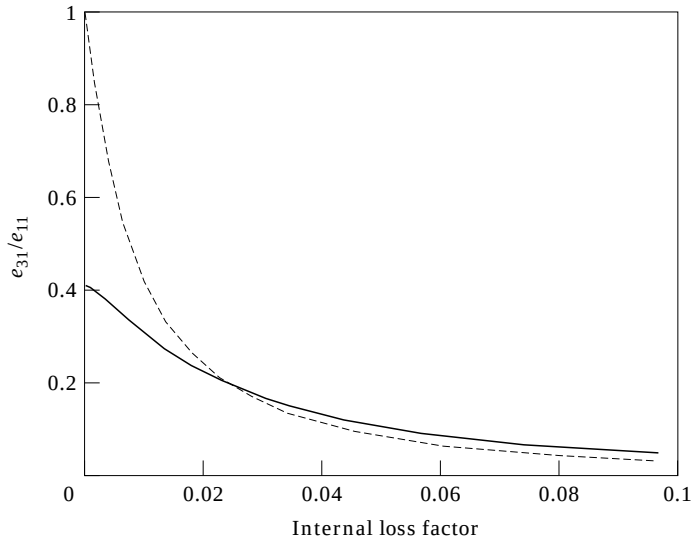

Figure 19. Ratio of modal energies e_{31}/e_{11} between plate 3 and plate 1. ——, Modal approach; – – –, wave approach.

region may very well be high. The changeover point beyond which the CLFs become insensitive to damping varies depending on the nature of the coupling as well as on the properties of the subsystems. It would be useful to be able to estimate the value of this changeover point, as it marks the beginning where statistical variances of SEA parameters becomes small. It is likely that the *modal overlap factor* might be a more informative variable to use than the internal loss factor, and that the changeover point should occur below an empirical modal overlap value of the order of unity. (Modal overlap factor = modal density × internal loss factor × $\omega\pi/2$. This measures the ratio of the average modal damping bandwidth to the average spacing between the modes.) This idea

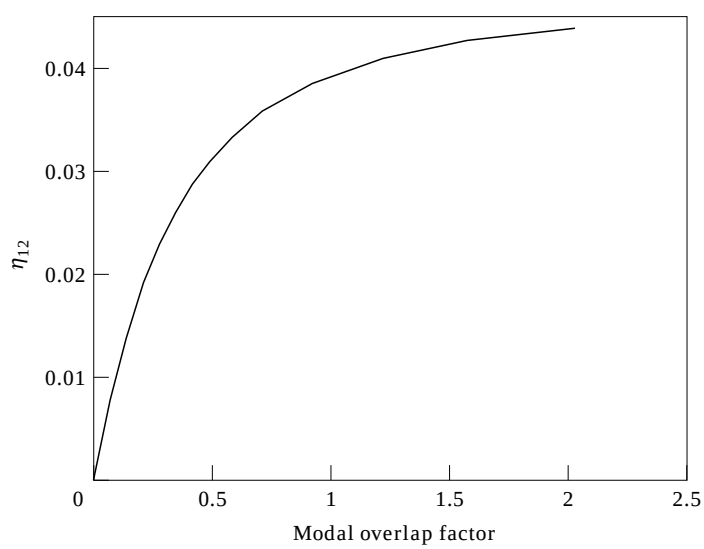

Figure 20. Coupling loss factors η_{12} plotted against modal overlap factors.

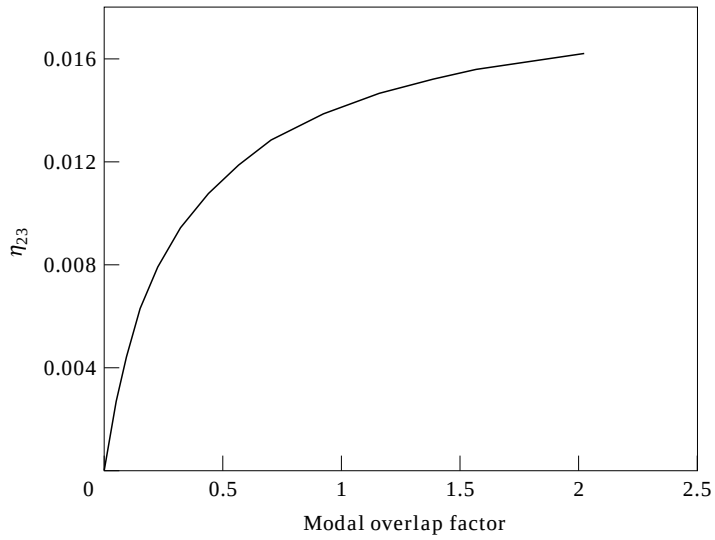

Figure 21. Coupling loss factors η_{23} plotted against model overlap factors.

is supported, for this particular system, by Figures 20 and 21 where the CLFs are plotted against the modal overlap factors. However, theoretical studies suggest that modal overlap will not in general be the only parameter which matters, and a more complicated formulation is probably necessary. A more extensive study of a wide variety of test systems would be described to explore this issue further.

Lastly, it should be pointed out that an extra source of complication is introduced by the presence of indirect coupling. The wave method only gives estimates for the direct CLFs η_{12} and η_{23}, which is effectively to assume the indirect CLF η_{13} to be zero. This means that the CLF matrix in equation (A4) is approximated by a banded matrix with three non-zero diagonals only. The errors introduced by this simplification will depend on the choice of the values of the direct CLFs (in the approximate matrix) and on which

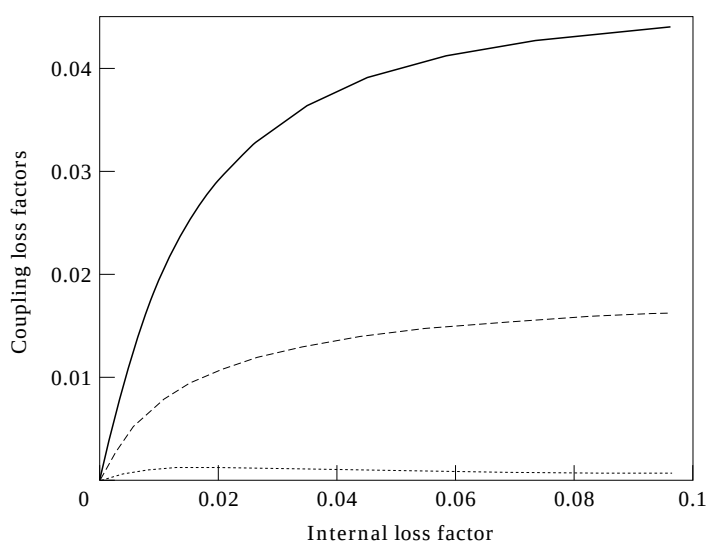

Figure 22. Direct and indirect CLFs for the three coupled plates. ——, η_{12}; – – –, η_{23}; · · · , η_{13}.

subsystem is being excited, as well as on the magnitude of the indirect CLFs (see Figure 22 for a comparison of CLFs for the three coupled plates).

7. CONCLUSIONS

The effects of damping on energy sharing in coupled systems have been investigated. It has been shown that the values of the coupling loss factors are in general strongly dependent on damping except when it is sufficiently high. (Exceptions might arise for special systems, such as those with identical subsystems.) For lightly damped coupled systems, varying the damping will cause the values of the coupling loss factors to vary in direct proportion to the internal loss factor. In the limit of zero damping, the coupling loss factors are equal to zero. This strong damping-dependency behaviour raises questions about the wave-transmission technique in estimating coupling loss factors. Since the wave approach does not relate damping to coupling loss factors, it is not clear to what damping levels the estimated values for the CLFs correspond. The usual assumption is that the wave technique is valid only for coupled systems with reasonably high modal overlap factors (equal to or greater than unity). This partly explains the common observation that the wave estimates generally exceed the actual values when the average modal overlap factors are small.

It is not obvious how the wave approach should be modified to allow for damping effects. Certainly, there should at least be some quantitative indicator to warn us when the wave predictions will be unreliable. One development in this area is described in the second edition of the SEA book by Lyon and DeJong [2, see Chapter 10]. Lyon and DeJong used a modal approach to derive the coupling loss factors for point connected and line connected subsystems. The formula for the CLF was expressed in terms of the wave transmission coefficients of the joint and an empirical 'correction factor' which accounts for low modal overlap effects. Another recent development which may be relevant in this context is the 'Advanced SEA' described by Heron [20].

One other implication of the strong damping-dependency behaviour is that the tendency towards equipartition of modal energy under low damping does not occur in general. This is contrary to the classical SEA prediction that equipartition of modal energy always occurs if the damping can be reduced to a sufficiently small value. It has been demonstrated that the use of this classical assumption can lead to gross overestimates of subsystem energy ratios, especially in multi-subsystem structures.

REFERENCES

1. J. Woodhouse 1981 *Applied Acoustics* **14**, 455–469. An introduction to statistical energy analysis of structural vibration.
2. R. H. Lyon and R. G. DeJong 1995 *Theory and Application of Statistical Energy Analysis*, (second edition). London: Butterworth-Heinemann.
3. C. H. Hodges and J. Woodhouse 1986 *Reports on Progress in Physics* **49**, 107–170. Theories of noise and vibration transmission in complex structures.
4. E. E. Ungar 1967 *Transactions of the American Society of Mechanical Engineers*, *Journal of Engineering for Industry*, *November*, 626–632. Statistical energy analysis of vibrating systems.
5. A. D. Mohammed and F. J. Fahy 1990 *Proceedings of the Institute of Acoustics* **3**, 543–550. A study of uncertainty in applications of statistical energy analysis to one-dimensional and two-dimensional structural systems.
6. F. J. Fahy and D. Y. Yao 1987 *Journal of Sound and Vibration* **114**, 1–11. Power flow between non-conservatively coupled oscillators.
7. A. J. Keane and W. G. Price 1987 *Journal of Sound and Vibration* **117**, 363–386. Statistical energy analysis of strongly coupled systems.

8. A. J. Keane and W. G. Price 1990 *Proceedings of the Institute of Acoustics*, **3**, 539–542. Exact power flow relationships between many multi-coupled, multi-modal sub-systems.
9. R. S. Langley 1989 *Journal of Sound and Vibration* **135**, 499–508. A general derivation of the statistical energy analysis equations for coupled dynamic systems.
10. G. Maidanik 1977 *Journal of Sound and Vibration* **52**, 171–191. Some elements in statistical energy analysis.
11. E. K. Dimitriadis and A. D. Pierce 1988 *Journal of Sound and Vibration* **123**, 397–412. Analytical solution for the power exchange between strongly coupled plates under random excitation: A test of statistical energy analysis concepts.
12. P. J. Remington and J. E. Manning 1975 *Journal of the Acoustical Society of America* **57**, 374–379. Comparison of statistical energy analysis power flow predictions with an exact calculation.
13. P. W. Smith, Jr., 1979 *Journal of the Acoustical Society of America* **65**, 695–698. Statistical models of coupled dynamic systems and the transition from weak to strong coupling.
14. C. H. Hodges, P. Nash and J. Woodhouse 1987 *Applied Acoustics* **22**, 47–69. Measurement of coupling loss factors by matrix fitting: An investigation of numerical procedures.
15. J. Woodhouse 1981 *Journal of the Acoustical Society of America* **69**, 1695–1709. An approach to the theoretical background of statistical energy analysis applied to structural vibration.
16. M. P. Norton 1989 *Fundamentals of Noise and Vibration Analysis for Engineers*, Cambridge University Press. See chapter 6, 371–427.
17. R. S. Langley 1992 *Journal of Sound and Vibration* **159**, 483–502. A wave intensity technique for the analysis of high frequency vibrations.
18. K. H. Heron 1994 *Philosophical Transactions of the Royal Society of London*, **A346**, 501–510. Advanced statistical energy analysis.
19. I. S. Gradshteyn and I. M. Ryzhik 1980 *Tables of Integrals*, *Series*, *and Products*. New York: Academic Press.
20. K. H. Heron 1990 *Proceedings of the Institute of Acoustics*, **3**, 551–556. The development of a wave approach to statistical energy analysis.
21. R. S. Langley and J. H. Heron 1990 *Journal of Sound and Vibration* **143**, 241–253. Elastic wave transmission through plate/beam junctions.
22. C. H. Hodges and J. Woodhouse 1989 *Journal of Sound and Vibration* **130**, 237–251. Confinement of vibration by one-dimensional disorder, I: theory of ensemble averaging.
23. C. H. Hodges and J. Woodhouse 1989 *Journal of Sound and Vibration* **130**, 253–268. Confinement of vibration by one-dimensional disorder, II: a numerical experiment on different ensemble averages.
24. D. E. Newland 1984 *An Introduction to Random Vibrations and Spectral Analysis*, (second edition). London: Longman.

APPENDIX A: SEA PARAMETERS IN TERMS OF FREQUENCY RESPONSE FUNCTIONS

Consider a system subjected to 'rain-on-the-roof' excitation on subsystem j with mean-square spectra density S_j which is constant within the frequency band Ω (and zero elsewhere).

The total mean energy of subsystem i, E_{ij}, is

$$E_{ij} = m_i S_j \int_{\Omega} \int_{\text{subsystem } i} \int_{\text{subsystem } j} |H(r, s, \omega)|^2 \, \mathrm{d}s \, \mathrm{d}r \, \mathrm{d}\omega, \qquad i = 1, \ldots, N, \tag{A1}$$

where m_i is the mass density of subsystem i. The input power Π_j is

$$\Pi_j = S_j \int_{\Omega} \int_{\text{subsystem } j} \mathrm{Re}[H(s, s, \omega)] \, \mathrm{d}s \, \mathrm{d}\omega, \qquad j = 1, \ldots, N. \tag{A2}$$

In matrix form,

$$\mathbf{\Pi} = \bar{\omega} \begin{bmatrix} (\eta_{11} + \eta_{12} + \cdots) & -\eta_{21} & -\eta_{31} & \cdots \\ -\eta_{12} & (\eta_{21} + \eta_{22} + \cdots) & & \\ -\eta_{13} & & \ddots & \\ \vdots & & & \end{bmatrix} \mathbf{E}, \tag{A3}$$

where $\mathbf{\Pi}$ is a diagonal matrix with diagonal entries given by equation (A2). Inverting this gives the coupling loss factor matrix

$$\mathbf{\Pi E}^{-1} = \bar{\omega} \begin{bmatrix} (\eta_{11} + \eta_{12} + \cdots) & -\eta_{21} & -\eta_{31} & \cdots \\ -\eta_{12} & (\eta_{21} + \eta_{22} + \cdots) & & \\ -\eta_{13} & & \ddots & \\ \vdots & & & \end{bmatrix}. \tag{A4}$$

APPENDIX B: INTEGRALS USED IN THE CALCULATION OF COUPLING LOSS FACTORS

$$\begin{aligned} \int \mathrm{Re}[H_j^* (\mathrm{i}\omega) H_k (\mathrm{i}\omega)]\, \mathrm{d}\omega = {} & \frac{A}{2} \tan^{-1}\left(\frac{\omega^2 - \omega_j^2}{\beta_j\, \omega}\right) \\ & + \frac{2B - A\beta_j}{4(\beta_j^2/4 - \omega_j^2)^{1/2}} \tan^{-1}\left(\frac{2\omega(\beta_j^2/4 - \omega_j^2)^{1/2}}{\omega^2 + \omega_j^2}\right) \\ & + \frac{A}{2} \tan^{-1}\left(\frac{\omega^2 - \omega_k^2}{\beta_k\, \omega}\right) + \frac{2C - A\beta_k}{4(\beta_k^2/4 - \omega_k^2)^{1/2}} \\ & \times \tan^{-1}\left(\frac{2\omega(\beta_k^2/4 - \omega_k^2)^{1/2}}{\omega^2 + \omega_k^2}\right), \end{aligned}$$

where

$$\begin{aligned} H_j (\mathrm{i}\omega) &= \mathrm{i}\omega/(-\omega^2 + \beta_j\, \mathrm{i}\omega + \omega_j^2), \\ A &= (\omega_j^2\, \beta_k + \omega_k^2\, \beta_j)/((\omega_j^2 - \omega_k^2)^2 + (\beta_j + \beta_k)\, (\omega_j^2\, \beta_k + \omega_k^2\, \beta_j)), \\ B &= (\omega_j^2\, (\omega_k^2 - \omega_j^2))/((\omega_j^2 - \omega_k^2)^2 + (\beta_j + \beta_k)\, (\omega_j^2\, \beta_k + \omega_k^2\, \beta_j)), \\ C &= (\omega_k^2\, (\omega_j^2 - \omega_k^2))/((\omega_j^2 - \omega_k^2)^2 + (\beta_j + \beta_k)\, (\omega_j^2\, \beta_k + \omega_k^2\, \beta_j)). \end{aligned}$$